Instabilities in a Liquid-Fluidized Bed of Gas Bubbles

M. U. Vera, A. Saint-Jalmes, and D. J. Durian

Departments of Physics & Astronomy, UCLA, Los Angeles, California 90095-1547
(Received 5 August 1999)

Gas bubbles in an aqueous foam can be unjammed, or fluidized, by introducing a forced flow of the continuous liquid phase at a sufficiently high rate. We observe that the resulting bubble dynamics are spatially inhomogeneous, exhibiting a sequence of instabilities vs increasing flow rate. First irregular swirls appear, then a single convective roll, and finally a series of stratified convection rolls each with a different average bubble size.

Sedimentation of particles in a liquid or gas caused by gravity, and fluidization caused by forced counterflow are important in many applied and geophysical situations, and are long-standing subjects of basic research. Intriguing questions concern fluctuations and instabilities, for example, the correlated swirling in sedimenting colloids [1,2] or the bubbling in gas-fluidized beds [3]. Sedimentation also occurs for gas bubbles in soapy water, i.e., for aqueous foams. There, the bubbles rise while the liquid drains down through the continuous random network of plateau borders, which then shrink in cross section [4,5]. In foam, a flow of liquid from above can propagate as a solitary wave [6,7] and cause both structural transitions [8] and large-scale convection [9].

When diffusion and direct interactions are negligible, the behavior of particles of diameter D and density ρ_p sedimenting at speed V in a fluid of density ρ_f and kinematic viscosity ν should be determined according to Reynolds numbers for particle and fluid. These are the ratios of inertial forces, $\rho_f V^2 D^2$ and $\rho_p V^2 D^2$, respectively, to viscous forces $\rho_f \nu V D \approx \Delta\rho g D^3$, all operating on a volume $\sim D^3$. This gives $\mathrm{Re}_f = V D/\nu = (\Delta\rho/\rho_f) g D^3/\nu^2$ and $\mathrm{Re}_p = (\rho_p/\rho_f)\mathrm{Re}_f$; the latter is also known as the Stokes number [10]. For colloidal solids in water, these numbers are $\mathrm{Re}_f \approx \mathrm{Re}_p \ll 1$; thus all motion is overdamped and large correlated swirling can be observed. For granular solids in air, the numbers are $\mathrm{Re}_f \sim 1$ and $\mathrm{Re}_p \sim 1000$; thus the grains experience rapid collisions and bubbling instabilities can be observed. The reciprocal holds for small gas bubbles in water, where $\mathrm{Re}_f \sim 1$ and $\mathrm{Re}_p \sim 10^{-3}$. This represents a relatively unexplored regime and, as we report here, the sequence of instabilities in response to fluidization can be dramatically different.

Experiment.—Foams are produced by turbulent mixing of N_2 gas metered into a fast jet of water containing 0.4% α-olefinsulfonate by weight [11]. This gives initial liquid fractions ε_0 that are uniform and adjustable from very dry to very wet, $0.03 < \varepsilon_0 < 0.40$. The bubble size distribution is polydisperse, but independent of ε_0. Roughly 60% of bubbles have radii between 40 and 70 μm, with none larger than 100 μm or smaller than 10 μm; the average radius is $R = 55$ μm. At time zero, foam is flowed from the production apparatus into a rectangular Plexiglas tank

that has several inches of surfactant solution on the bottom (see Fig. 1). A vertical divider extends into the solution, such that the foam on one side is in hydrostatic equilibrium with displaced solution on the other. The ratio of liquid displacement to foam height equals the average liquid fraction, $\langle\varepsilon\rangle$, similar to the method of Ref. [9]. The foam sample is 35 cm tall with a cross section A of 21.6 cm wide by 1.27 cm thick (8.5 in. × 1/2 in.). To achieve a uniform nonpulsatile counterflow of liquid, a magnetically coupled gear pump takes surfactant solution from the bottom of the tank and returns it at the top through a manifold of drip heads spaced 1.27 cm apart and just immersed into the foam.

Free drainage.—The strength of the forced counterflow is gauged by comparison with the rate of free drainage. Results for $\langle\varepsilon\rangle$ vs time are shown in Fig. 2 by heavy solid curves for foams with $\varepsilon_0 = 0.09$, 0.15, and 0.26; these data are identical to those obtained previously from the height of drained liquid [11]. Initially, the rate of downward flow is uniform throughout the column and is set only by gravity and dissipation. Consequently the foam first becomes dry at the top, with a "drying front" that propagates downward at 2 to 3 times the speed of the flowing liquid [11]. For the wettest foams, the drained liquid emerges almost immediately; for drier foams, however, capillarity prevents leakage until the liquid fraction at the bottom of the sample increases to about $\varepsilon_c \approx 0.37$, at which point the bubbles are randomly packed spheres. We measure the maximum rate, Q_m, at which drained liquid emerges, and then normalize by the cross section A of
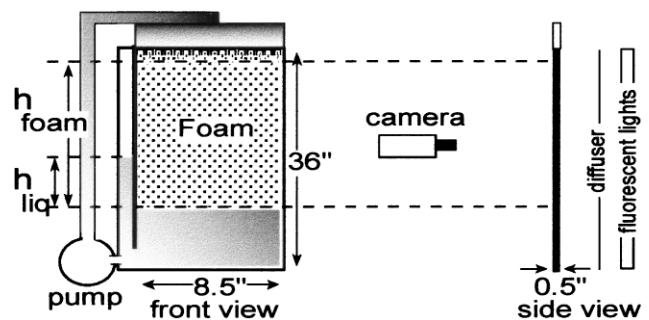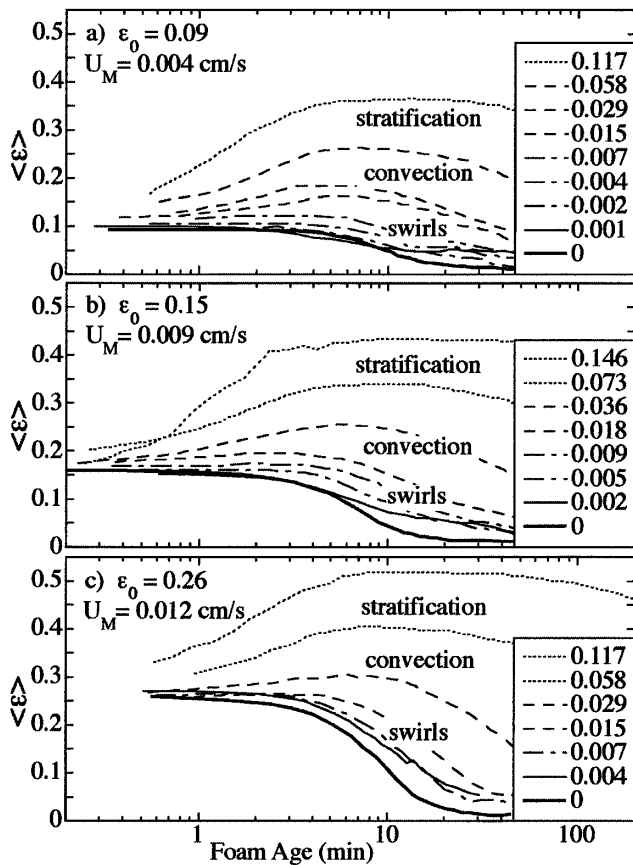

FIG. 1. Schematic view of fluidized bed.

FIG. 2. Average liquid fraction vs time for three different initial liquid fractions, ε_0, and many forced flow rates, $U = Q/A$, as labeled. The heavy solid curves are for no flow, where the maximum "free drainage" rate is U_m. The light solid curves are for slow flows, $U < U_m/2$, where the bubbles remain jammed. The dot-dashed curves are for intermediate flows, $U_m/2 < U < U_m$, where irregular *swirls* are observed. The dashed curves are for higher flows, $U > U_m$, where a single *convection* roll is found. And the dotted curves are for the highest flow rates, such that $\langle \varepsilon \rangle > 0.30$, where *stratified* convection plus size segregation is found.

the foam; the resulting maximum superficial flow speeds, $U_m = Q_m/A$, increase with ε_0 as labeled in Fig. 2. At later times, drainage and leakage proceed at a slower and slower pace until an equilibrium liquid fraction gradient is established in which gravity is balanced by capillarity. This entire sequence may be described by a nonlinear partial differential "drainage equation" [4,12], though quantitative agreement is still lacking with experiment [11].

Low flow.—We now explore response vs the rate $U = Q/A$ at which liquid is pumped from above. For the lowest rates, $U < U_m/2$, the bubbles remain jammed in their initial configuration and the extra liquid simply percolates down through the fixed network of plateau borders. Therefore, the average liquid fraction decreases less slowly than for free drainage, as can be seen by the thin solid curves in Fig. 2. This could presumably be described by the drainage equation, but the solutions are not known. Our situation is slightly different from the usual case of a wet-

ting front propagating into a dry foam [6,7]. There, flow occurs only behind the wetting front. Here, flow occurs throughout the entire foam, with the imposed wetting front traveling more slowly than the free-drainage drying front.

Intermediate flow.—As the forcing exceeds $U_m/2$, we observe a sequence of convective instabilities. The first, for counterflows between $U_m/2$ and roughly U_m, consists of irregular swirls as depicted in Fig. 3(a). Here the darker regions correspond to wetter regions of foam, which flow into the drier lighter regions. One can also see from Fig. 2 that this is important in transporting liquid: forcing at $U < U_m/2$, where there is no convection, actually causes the foam to retain liquid longer than forcing at higher rates. For every repetition of this experiment we observe the same $\langle \varepsilon \rangle$ response but a different pattern of swirls, with no discernible large-scale organization. This rules out any bias due to slight differences in the flow rate from each drip head. The swirls can be due to only an intrinsic instability of the wetting front as it invades the foam. If one could solve the drainage equation for the low-flow case above, it might be possible to do a linear stability analysis to identify the onset at which fluctuations grow rather than shrink with time. It seems natural that such an instability exists: if a portion of the front becomes wetter by fluctuation, then the plateau borders necessarily become thicker and the flow should increase at the expense of the rest of the front. It also seems natural that U_m sets the scale beyond which convection occurs. For slower flows, the free-drainage drying front travels faster than the imposed wetting front. For faster flows, the wetting front overtakes the drying front, which causes a progressive buildup of liquid at the top of the foam. Furthermore, this is similar to what happens in colloids or granular media: when the forcing is more rapid than the rate at which the particles sediment, then drag from the counterflow overcomes gravity and the system fluidizes. One then sees bubbles in gas-fluidized beds of solids, and swirling in liquid-fluidized beds of solids or gas bubbles.

As the forcing is increased further, the next qualitative change occurs at approximately $U > U_m$. Here, the swirling organizes into a single convection roll as depicted in Fig. 3(b). The darker, wetter side of foam falls, dropping off liquid at the bottom of the tank while the lighter, drier side rises. The rotation direction locks in as clockwise or counterclockwise at random. Concurrent behavior of $\langle \varepsilon \rangle$ vs time is shown in Fig. 2. At first the liquid content increases while the foam swells and the wet swirls stir the system randomly. Next the foam becomes more homogeneously wet, before a roll organizes and shifts the wetness to one side. The liquid fraction then reaches a maximum, before slowly decreasing as the bubbles coarsen and allow liquid to pass through more rapidly.

Convection was reported earlier, but for foams with 0.5–5 mm diameter bubbles individually blown into 10–20 mm diameter cylinders [9]. There, no swirling precursor was reported. Also, no comparison could be
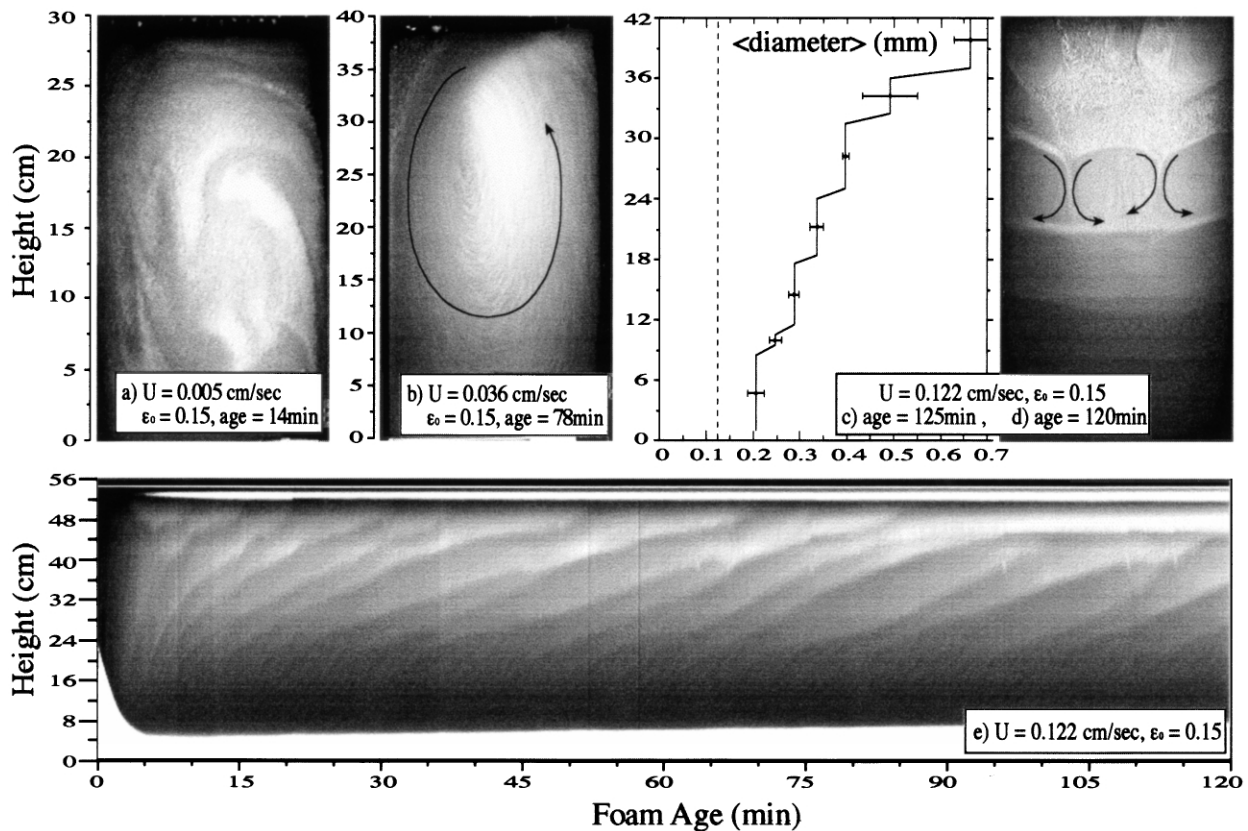
FIG. 3. Swirling (a), convection (b), and size segregation plus layered convection (c)–(e). The initial liquid fraction is $\varepsilon_0 = 0.15$, and counterflow rates are labeled.

made with initial liquid fraction or free-drainage rate owing to production method. Futhermore, U_m must decrease for smaller bubbles, but larger counterflows were needed for onset of convection. Consistency with our observations requires either that the size or shape of the sample be important or that there be an unknown variation of their initial liquid fractions with bubble size. When our tank width is reduced to 0.5 in., equal to the depth, we find no convection and no vertical gradients in wetness or bubble size at superficial flow speeds that cause a single large roll in the 8.5 in. wide tank.

High flow.—At the very highest rates of counterflow we find a dramatic secondary instability, shown in Fig. 3(d). Here the system organizes into stratified layers each with several counterrotating rolls. Adjacent layers may convect, or a narrower stagnant region may intervene. From top to bottom, the layers become progressively wetter and hence appear darker. Further enhancing this contrast, the average bubble size progressively decreases from top to bottom, as shown in Fig. 3(c). At the bottom layers, we see a rapidly seething froth of tiny bubbles, and a diffuse interface with the drained liquid underneath. We emphasize that the initial size distribution, while polydisperse, was uniform throughout the foam. The size segregation at high flows is part of a rich dynamics, coupled closely to the layered convection.

Inspection of Fig. 2 shows that layered convection with size segregation occurs when the forced counterflow exceeds about $U = 0.060$ cm/s and $\langle \varepsilon \rangle$ exceeds about 0.30. This is close to the value $\varepsilon_c = 0.37$ at which the bubbles become randomly close packed spheres, and beyond which they unjam and the bulk elastic properties vanish [13]. So whereas the initial instabilities are located by comparison of U with the maximum rate U_m of free drainage, the secondary instability of Fig. 3(d) is located where the foam becomes sufficiently wet that the bubbles are free to rearrange in response to the various forces.

The size and structure of rotating rolls depends on the sample dimensions. To see this we progressively reduced the width of our tank, maintaining the same fixed superficial flow speed of $U = 0.122$ cm/s onto foams with initial liquid fractions of $\varepsilon_0 = 0.15$. When cut to 4 in. across, we find two counterrotating rolls of 2 in. diameter, the same size as the four rolls in Fig. 3(d). When cut to 2 in., we still find two counterrotating rolls but of 1 in. diameter. When cut to 1 in., we find a stack of single rolls of 1 in. diameter all rotating in the same direction. And when cut to 0.5 in., equal to the sample depth, we find a vertical wetness and bubble size gradient but no discernible convection.

It may be instructive to compare with related phenomena in other systems. In particular, the formation of sharp layers in sedimenting suspensions has been reported for many

kinds of particles. This is reviewed in Ref. [14], where layering was attributed to spinodal decomposition. A different explanation was advanced in terms of shock fronts of the Burgers equation [15]. This may be relevant to foams, in that the drainage and Burgers equations are both nonlinear partial differential equations expressing mass conservation for systems that sediment/drain more rapidly when the particles/bubbles are more dilute. However, this cannot account for the observed coupling with convection. Layered structures have also been found in "creaming" emulsions [16]. There, the layers were not shock fronts, but rather convection rolls caused by a slight horizontal temperature gradient across the thin dimension of the sample. Here, we are unable to generate convection by thermal gradients. Also, our rolls counterrotate with axes perpendicular to the sample face, whereas in [16] they all rotate in the same direction with axes parallel to the face.

Visual inspection reveals three possible mechanisms for size segregation. First, very small bubbles can be flushed downward by liquid percolating in between large slowly convecting bubbles. Second, small bubbles can be dropped off at the bottom, and large bubbles at the top, of the convection rolls. This is reminiscent of the "Brazil nut effect" in which large grains separate from small grains under shaking-induced convection [17]. And last, the bubble size distribution can coarsen by the diffusion of gas from smaller to larger bubbles. Comparing the vertical line in Fig. 3(c) for the initial average bubble diameter with those for the layered structure at age 120 min shows that bubbles have coarsened as well as segregated. If a layer has larger bubbles, it will pass the liquid more rapidly and hence become drier; once drier, it will coarsen even more rapidly because the gas transport between neighboring bubbles is correspondingly faster. This enhances size segregation but does not seem responsible for its original occurrence. In Fig. 3(e), a space-time plot depicts the time evolution of the system. The layering and segregation appear within minutes, before the size distribution could noticeably change. As coarsening proceeds, the layers rise and disappear at the top while new ones form at the bottom.

Conclusion.—In summary, we have described the series of instabilities induced by a fluidizing counterflow of liquid downward through a bed of gas bubbles. Originally we had hoped for a homogeneous response, so that very wet (albeit steadily draining) foams could be studied in earth's gravity without change of liquid fraction; in this sense, our experiments were a spectacular failure. When the flow rate per unit cross section, $U = Q/A$, is below half the maximum rate U_m for free drainage, then the bubbles remain jammed and the liquid drains exclusively by percolation through the fixed random network of plateau borders. When the rate is between $U_m/2$ and roughly U_m, then some portions of the foam become sufficiently wet to

fluidize in the form of irregularly shaped flowing swirls. For higher rates, the entire foam fluidizes in the form of a single system-wide convection roll. And finally when the rate is so great that the average liquid content exceeds that required for the bubbles to be randomly close packed spheres, then layered convection rolls appear, each with a different average bubble size. To understand such rich dynamics may require that the drainage equation be supplemented by mechanisms for convective transport of liquid along with flowing bubbles; spatial and temporal variation of the size distribution may also be needed. This could lead to improved processing of foamed materials or of introducing additives to break unwanted foams. It could also complement a fuller understanding of related instabilities in the sedimentation and fluidization of solid particles.

[1] P. N. Segre, E. Herbolzheimer, and P. M. Chaikin, Phys. Rev. Lett. **79**, 2574 (1997).

[2] A. Levine, S. Ramaswamy, E. Frey, and R. Bruinsma, Phys. Rev. Lett. **81**, 5944 (1998).

[3] N. Menon and D. J. Durian, Phys. Rev. Lett. **79**, 3407 (1997).

[4] D. Weaire, S. Hutzler, G. Verbist, and E. Peters, Adv. Chem. Phys. **102**, 315 (1997).

[5] A. Bhakta and E. Ruckenstein, Adv. Colloid Interface Sci. **70**, 1 (1997).

[6] D. Weaire, N. Pittet, S. Hutzler, and D. Pardal, Phys. Rev. Lett. **71**, 2670 (1993).

[7] S. A. Koehler, S. Hilgenfeldt, and H. A. Stone, Phys. Rev. Lett. **82**, 4232 (1999).

[8] N. Pittet, P. Boltenhagen, N. Rivier, and D. Weaire, Europhys. Lett. **35**, 547 (1996).

[9] S. Hutzler, D. Weaire, and R. Crawford, Europhys. Lett. **41**, 461 (1998).

[10] D. L. Koch, Phys. Fluids A **2**, 1711 (1990).

[11] A. Saint-Jalmes, M. U. Vera, and D. J. Durian, Eur. Phys. J. B **12**, 67 (1999).

[12] S. A. Koehler, H. A. Stone, M. P. Brenner, and J. Eggers, Phys. Rev. E **58**, 2097 (1998).

[13] A. Saint-Jalmes and D. J. Durian, J. Rheol. **43**, 1411 (1999).

[14] D. B. Siano, J. Colloid Interface Sci. **68**, 111 (1979).

[15] W. van Saarloos and D. A. Huse, Europhys. Lett. **11**, 107 (1990).

[16] D. M. Mueth, J. C. Crocker, S. E. Esipov, and D. G. Grier, Phys. Rev. Lett. **77**, 578 (1996).

[17] J. B. Knight, H. M. Jaeger, and S. R. Nagel, Phys. Rev. Lett. **70**, 3728 (1993).

[18] S. Hutzler, D. Weaire, and S. Shah, Philos. Mag. Lett. **80**, 41 (2000).